Evaluation of Techniques for Predicting Static Aeroelastic Effects on Flexible Aircraft

IRVING ABEL*
NASA Langley Research Center, Hampton, Va.

An experimental evaluation of analytical techniques for predicting the longitudinal stability characteristics of a large flexible aircraft is presented. Analytical methods based on both the modal approach and stiffness influence coefficients are used to predict the aerodynamic characteristics of a flexible airplane. These methods are then applied to a flexibly scaled model of a supersonic transport configuration. Comparisons between wind-tunnel data, the modal approach, and calculations based on stiffness influence coefficients are presented over the Mach number range from $M = 0.6$–2.7. The results of this study show good agreement for most cases between analyses and experiment.

Nomenclature

a.c. = aerodynamic center position
Δa.c. = shift in aerodynamic center position due to flexibility, positive forward
b = wing span
c = local chord measured streamwise
$\bar{c}$ = reference chord
C_L = lift coefficient, lift/qS
$C_{L\alpha}$ = lift-curve slope, $\partial C_L/\partial\alpha$ at $\alpha = 0°$
$C_L|_{\alpha=0}$ = lift coefficient at $\alpha = 0°$
C_{Lq} = lift coefficient due to pitching, $\partial C_L/\partial(\dot{\theta}\bar{c}/2V)$
$C_{L\delta_e}$ = elevator effectiveness in lift, $\partial C_L/\partial\delta_e$
C_m = pitching-moment coefficient, pitching moment/$qS\bar{c}$ †
$C_{m\alpha}$ = static stability derivative, $\partial C_m/\partial\alpha$ at $\alpha = 0°$
$C_{m\delta_e}$ = elevator effectiveness in pitch, $\partial C_m/\partial\delta_e$
$C_m|_{\alpha=0}$ = pitching-moment coefficient at $\alpha = 0°$
C_{m_q} = pitching moment due to pitching, $\partial C_m/\partial(\dot{\theta}\bar{c}/2V)$
C_N = normal-force coefficient, normal force/qS
$C_{N\alpha}$ = normal-force curve slope, $\partial C_N/\partial\alpha$ at $\alpha = 0°$
F = deflection per unit load
$H(x,y)$ = vertical displacement of point x, y
$h_i(x,y)$ = shape of the ith vibration mode of model structure
I = mass moment of inertia in pitch
M = airplane total mass
$m(x,y)$ = mass distribution of flexible model
M_i = generalized mass of the ith vibration mode
N_i = normal force per unit generalized displacement
n = load factor, lift/weight
P_i = pitching moment per unit generalized displacement
ΔP = lifting pressure over wing
ΔP_i = pressure distribution due to downwash of the ith mode, per unit generalized coordinate
q = freestream dynamic pressure
q_i = generalized coordinate of ith vibration mode
$\bar{q}_i$ = generalized coordinate per unit angle of attack, q_i/α
Q_i = ith mode generalized force
S = reference wing area
V = freestream velocity
$w(x,y)$ = downwash velocity on wing
x,y,z = orthogonal coordinate system, body axis
Z_{mcl} = coordinate of mean-camber line, $(z_{upper} + z_{lower})/2$
α = angle of attack measured from wing reference plane
δ_e = wing trailing-edge control displacement in pitch, positive for trailing edge down
ω_i = frequency of the ith structural mode

Subscripts

A = full-scale airplane
flex = flexible model
m = model
rigid = rigid model

I. Introduction

SOME effects of aeroelasticity on aircraft design have been considered for many years. However, with the general class of aircraft to date, the primary concern has been with such problems as flutter, response to turbulence, control effectiveness, and so forth. Now that we are entering the era of large supersonic aircraft with their increased size, speed, and flexibility, the effect of aeroelasticity on static aerodynamic characteristics has also become an area of major concern.

At present no thorough experimental evaluation of analytical approaches to the problem are available for a supersonic transport configuration with its inherently more flexible characteristics. Recent papers by Roskam,[1] and Dusto and Chevalier[2] present comparisons between theory and experiment, but these are limited by the flexibility of the model investigated. Recognizing the need for definitive comparisons between calculated and measured wind-tunnel data, NASA Langley Research Center, in cooperation with the Boeing Company, undertook a comprehensive program employing both a rigid and flexibly scaled model of a recent supersonic transport configuration.

As part of this program, an analysis to predict the effect of flexibility on the longitudinal aerodynamic characteristics was developed at Langley, using a modal approach, similar to that described by Wykes.[3] The basic modal approach has been widely used in the field of aircraft structural dynamics, and the adaptation of this method to the static problem, utilizing the same unsteady aerodynamic theories already available for flutter and other dynamic calculations, provided a convenient framework. Analytical calculations employing an influence coefficient approach were made by the Boeing Company.‡ Results obtained from both analytical techniques are presented and compared with experiment.

The experimental portion of the program utilized separate 0.015 size rigid and flexibly scaled models. A complete description of the flexible model would merit a separate paper; therefore, only a brief description of the construction and design philosophy is included. Data from wind-tunnel tests collected at Mach numbers from 0.6–2.7 over a range of dynamic pressures from 250 to 1000 psf are presented and compared with analyses.

Received April 6, 1971; presented as Paper 71-343 at the AIAA/ASME 12th Structures, Structural Dynamics and Materials Conference, Anaheim, Calif., April 19–21, 1971; revision received August 26, 1971.

Index categories: Aircraft and Component Wind-Tunnel Testing; Structural Static Analysis; Aeroelasticity.

* Aerospace Engineer, Aeroelasticity Branch, Loads Division. Member AIAA.

† Moment reference center is located at 45% of $\bar{c}$ (Fig. 1).

‡ Unpublished data obtained from R. C. Schwanz, the Boeing Co., Seattle, Wash.

It is important to mention that the results presented are not directly applicable to a full-scale airplane since they do not include inertia effects. The results presented are, in effect, "massless airplane characteristics" since the model experiences a constant ($n = 1$) load factor and the balance of gravitational forces with aerodynamic forces (Froude number) was not scaled. However, this is not a serious problem, since the main purpose of the program is to evaluate analytical approaches and both analytical techniques have the ability to include these inertia loadings.

II. Description of Models and Test Apparatus

Rigid Model Description

The shape of the rigid model is dictated by performance and defined as the shape of the airplane "frozen" at $1g$ cruise ($M = 2.7$). This shape was predetermined at NASA Langley and used as a basis for all wind-tunnel tests. A drawing of the complete model configuration is shown in Fig. 1. The 0.015 size solid steel model incorporates a slender cambered body with a 74° swept-wing planform, four simulated engine nacelles, two vertical tails, and movable control surfaces. The swept-wing planform has a subsonic leading edge except in the region of the tip where the leading-edge sweep is reduced to 65°.

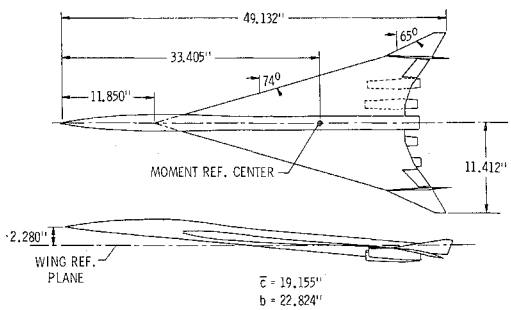

Fig. 1 Details of model.

Flexible Model Description

The flexible model was designed from the shape of the rigid model at cruise ($M = 2.7$, $C_L = 0.09$, $q_A = 540$ psf). The 0.015 size flexible model was elastically scaled with a rigid forward fuselage and elastic wings and aft fuselage. The condition for model similarity, as given in Ref. 1, is that

$$q_m/q_A \, F_m/F_A \, S_m/S_A{}^{1/2} = 1.0$$

The wings and aft fuselage were built according to this scaling rule. A dynamic pressure ratio (q_m/q_A) of 1.20 was selected to insure comparable flight dynamic pressures with those available in the wind tunnel. In order to simulate aerodynamic characteristics of the flexible airplane, it is only necessary to scale static load deflections; therefore, model weight was not scaled. A photograph of the model prior to testing is shown in Fig. 2.

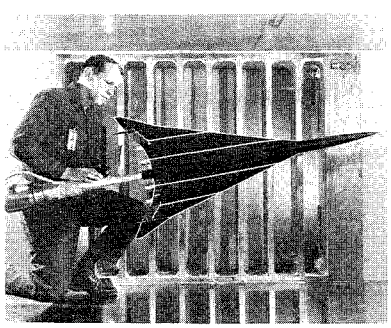

Fig. 2 Photograph of flexible model.

The flexible model was built so that at the design point the shape of the rigid and flexible models is the same. In order to achieve this, the flexible model is constructed to a model jig shape that is defined as the shape of the model when aerodynamic loads at the design point are removed. (The model jig shape will differ from that of the airplane jig shape since neither airplane mass nor mass distribution is simulated.) Figure 3 shows a typical comparison of the mean-camber line between cruise shape and the corresponding jig shape at span station $y/(b/2) = 0.68$. It may be noted that differences in the two shapes are substantial.

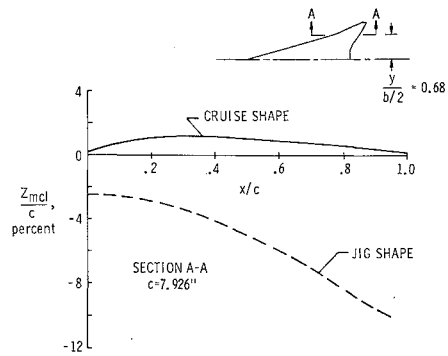

Fig. 3 Comparison of mean-camber line for rigid and flexible models at wing station $y/(b/2) = 0.68$.

Construction of the flexible model was achieved by using a structural layout that would be quite similar to that of a full-scale airplane. Structural ribs were fabricated from a balsa wood and fiberglas sandwich with a thin aluminum cap. Foam was used between structural members to provide the proper wing contour. Finally, fiberglas skins were bonded to the upper and lower surfaces to provide the properly scaled stiffnesses. Figure 4 shows a photograph of the basic model structure during construction. The flexible model was designed and constructed by the Boeing Company.

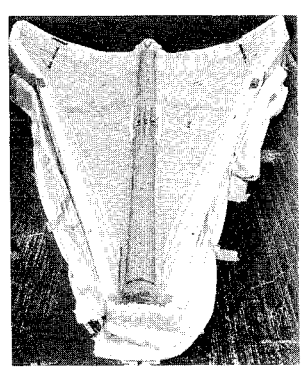

Fig. 4 Photograph of flexible model during construction.

Model Properties

For the modal analysis, it was necessary to experimentally determine a set of generalized masses, mode shapes, and natural frequencies. These properties were measured for the first five symmetric structural modes of the model. Generalized masses were determined using the method of displaced frequencies.[4] An experimentally measured flexibility matrix was used in the influence coefficient analysis. Both sets of measurements were made for a sting-mounted model.

Test Apparatus

The wind-tunnel studies were conducted in the Langley 8-ft transonic pressure tunnel and the Langley Unitary Plan wind tunnel in order to obtain aeroelastic data at high

dynamic pressure. Aerodynamic forces and moments were measured using a six-component strain-gage balance mounted within the model. Angle-of-attack was corrected for tunnel flow angularity and for deflection of the sting and balance under aerodynamic load. Identical boundary-layer transition strips were used on both models. Reynolds number varied from 1.1×10^6 to 5.2×10^6/ft over the Mach number range investigated.

III. Aeroelastic Analysis Techniques

Analytical calculations for the rigid model as a function of Mach number and for the flexible model as a function of Mach number and dynamic pressure have been made by the Boeing Company employing influence coefficients and by Langley employing the modal approach. Since the influence coefficient approach is amply described in the literature,[5] only a brief description of the modal approach is presented.

Modal Technique

A digital computer program, using the approach discussed in Ref. 3, was developed at Langley to predict aeroelastic effects on longitudinal stability and control characteristics. Under the following assumptions: 1) forward airspeed V is constant, 2) angle-of-attack is small ($C_N \approx C_L$), 3) small structural deformation, 4) structural acceleration and structural velocity negligibly small, the linearized free-flight longitudinal equations of motion appear in a general form as follows: (body axis)

$$M_i\ddot{q}_i(t) + \omega_i^2 M_i q_i(t) = Q_i(t) \tag{1}$$

where

$$M_i = \int_S \int h_i^2(x,y)m(x,y)ds$$

$$Q_i(t) = \int_S \int Z(x,y,t)h_i(x,y)ds$$

$$Z(x,y,t) = \Delta P(x,y,t) - ngm(x,y)$$

$$\Delta P(x,y,t) = \sum_{i=1}^{n} \Delta P_i(x,y,t)q_i(t)$$

It is assumed that the displacement of the wing can be represented by a superposition of the normal modes of oscillation, so that

$$H(x,y,t) = h_1(x,y)q_1(t) + h_2(x,y)q_2(t) + \cdots + h_n(x,y)q_n(t)$$

where q_i is the magnitude of the ith mode, and $h_i(x,y)$ gives the shape of the ith mode. The downwash velocities at any point on the wing surface are expressed as

$$w(x,y) = V\,\partial H(x,y,t)/\partial x + \dot{H}(x,y,t)$$

Letting h_1 be the rigid body plunge, h_2 rigid body pitch, $\dot{\theta} = 0$, and using assumption 4), we have

$$q_1 = z \quad q_2 = \theta \quad h_1 = 1 \quad h_2 = x$$

The downwash may now be expressed as

$$w(x,y) = V\left\{\sum_{i=3}^{n} \frac{\partial h_i(x,y)}{\partial x} q_i + \alpha\right\}$$

where

$$\alpha = \theta + \dot{z}/V$$

The aerodynamic loading is composed of two parts, namely

$$V\sum_{i=3}^{n} \frac{\partial h_i}{\partial x} q_i = \text{flexible load} \quad V\alpha = \text{rigid load}$$

Once the downwash is known over the wing, the pressure distribution can be readily obtained from available aerodynamic theories.[6,7] In the modal framework, pressure distributions are determined from modes in the following manner:

$$\begin{matrix}\text{modes} \\ (h_i)\end{matrix} \rightarrow \begin{matrix}\text{aerodynamic} \\ \text{program}\end{matrix} \rightarrow \begin{matrix}\text{pressure distribution} \\ (\Delta P_i)\end{matrix}$$

Using free-free normal modes (both rigid body and structural) the longitudinal equations of motion are written as

$$M\ddot{z} = q_3 \int_S \int \Delta P_3 ds + \cdots + q_n \int_S \int \Delta P_n ds + \alpha \int_S \int \Delta P_\alpha ds - Mgn \tag{2a}$$

$$I\ddot{\theta} = q_3 \int_S \int x\Delta P_3 ds + \cdots + q_n \int_S \int x\Delta P_n ds + \alpha \int_S \int x\Delta P_\alpha ds \tag{2b}$$

$$\omega_3^2 M_3 q_3 = q_3 \int_S \int h_3 \Delta P_3 ds + \cdots + q_n \int_S \int h_3 \Delta P_n ds + \alpha \int_S \int h_3 \Delta P_\alpha ds \tag{2c}$$

$$\vdots$$

$$\omega_n^2 M_n q_n = q_3 \int_S \int h_n \Delta P_3 ds + \cdots + q_n \int_S \int h_n \Delta P_n ds + \alpha \int_S \int h_n \Delta P_\alpha ds \tag{2n}$$

Normal force and pitching-moment forces per unit generalized displacement are defined from Eqs. (2a) and (2b) as

$$N_i = \int_S \int \Delta P_i ds, \qquad P_i = \int_S \int x\Delta P_i ds$$

Once the generalized mass M_i and the aerodynamic forces Q_i are evaluated, Eqs. (2c–2n) are solved simultaneously for the generalized displacement q_i per unit angle of attack α, $\bar{q}_i$. Once $\bar{q}_i$ is determined, the flexible aerodynamic characteristics are written as

$$(C_{L_\alpha})_{\text{flex}} \approx (C_{N_\alpha})_{\text{flex}} = (1/qS)\,[\bar{q}_3 N_3 + \bar{q}_4 N_4 + \cdots + \bar{q}_n N_n] + (C_{N_\alpha})_{\text{rigid}}$$

$$(C_{m_\alpha})_{\text{flex}} = (1/qS\bar{c})\,[\bar{q}_3 P_3 + \bar{q}_4 P_4 + \cdots \bar{q}_n P_n] + (C_{m_\alpha})_{\text{rigid}}$$

In a similar manner the other aerodynamic coefficients such as $C_L|_{\alpha=0}$, $C_m|_{\alpha=0}$, $C_{m_{\delta e}}$, $C_{L_{\delta e}}$, C_{L_q}, C_{m_q} can be evaluated by using the appropriate rigid loading.

Calculations were made for a sting-mounted model using the first five measured symmetric modes and generalized masses. The basic free-flight equations represent the constrained model if we assume that integrals of the form

$$\int_S \int m(x,y)h_i(x,y)ds$$

and

$$\int_S \int m(x,y)h_i(x,y)h_j(x,y)ds \qquad i \neq j$$

are negligibly small. The aerodynamics used to calculate the generalized aerodynamic forces were formulated through the use of a kernel function[6] procedure subsonically and a Mach Box[7] procedure supersonically. Only the wing is represented aerodynamically.

Influence Coefficient Technique (I.C. Analysis)

A digital computer program described in Ref. 5 was developed by the Boeing Company to predict aeroelastic effects on stability and control characteristics. The program combines aerodynamics, structural flexibility, and airplane geometry to calculate these effects.

Calculations were made, using this technique, for a kinematically constrained model by means of an experimentally measured flexibility matrix. The aerodynamic representation of the model was formulated by constant pressure vortex panels[8] and included the forebody, wing, and cylindrical aft body.

IV. Results

In this section a comparison between longitudinal results obtained with the rigid model, flexible model, and theoretical calculations will be discussed.

A comparison of the results of analytical calculations and wind-tunnel data in predicting the variation of lift-curve slope and aerodynamic center location with Mach number is presented in Fig. 5. Results are given for both the rigid model and flexible model at a dynamic pressure of 500 psf. The effect of dynamic pressure at all Mach numbers is to reduce C_{L_α} significantly and shift the aerodynamic center in the forward destabilizing direction. At $M = 1.2$ the largest effect of dynamic pressure occurs, resulting in reductions of C_{L_α} of approximately 37% and shifts in the aerodynamic center of about 18% of $\bar{c}$. Changes in the aerodynamic center are associated with bending deflections outboard on the wing which tends to reduce the local angle-of-attack; subsequently, its contribution to the total wing lift is reduced, resulting in a forward shift. In general, correlation between analyses and experiment is reasonable.

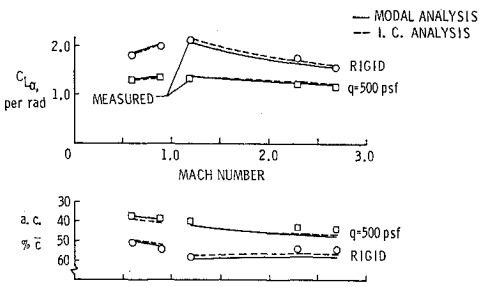

Fig. 5 Variation of lift-curve slope and aerodynamic center location with Mach number.

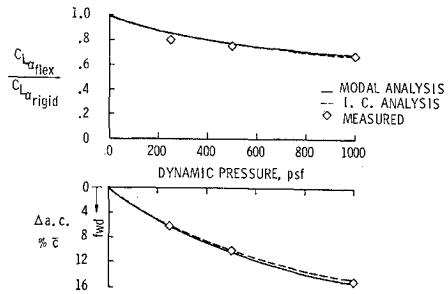

Fig. 6 Effect of dynamic pressure on measured and calculated flexible to rigid C_{L_α} ratio and aerodynamic center movement at $M = 2.7$.

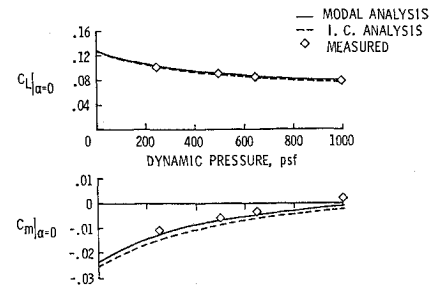

Fig. 7 Effect of dynamic pressure on measured and calculated $C_L|_{\alpha=0}$ and $C_m|_{\alpha=0}$ at $M = 2.7$.

Typical correlations of the ratio of C_{L_α} flexible to rigid and change in aerodynamic center between both the model and calculations, over a range of dynamic pressure, at $M = 2.7$ are presented in Fig. 6. These data are typical of that collected at other Mach numbers. It is noted from this figure that both analyses predicted the effect of dynamic pressure on C_{L_α} and aerodynamic center quite well even though neither predicted the absolute position of the aerodynamic center location at this Mach number (see Fig. 5).

Figure 7 presents a comparison of lift and pitching-moment coefficients at $\alpha = 0°$ with dynamic pressure for $M = 2.7$. It can be seen from this figure that agreement for lift coefficient is quite good, while the pitching-moment coefficient is predicted less well. However, both analyses did predict the increments in pitching-moment coefficient due to dynamic pressure somewhat closer. It should be mentioned that for the data presented so far, the comparison between influence coefficient analysis and modal analysis has been quite comparable even though both analyses were run independently, using different structural and aerodynamic representations of the model.

The effect of flexibility on pitch-control effectiveness for trailing-edge controls at $M = 2.7$ is presented in Fig. 8. The correlation between experiment and analyses is quite poor in predicting the absolute level. However, the increment in control effectiveness with dynamic pressure is predicted somewhat closer. It is believed that part of this problem is due to the inadequacy of either aerodynamic theory to properly predict the rigid loading due to the proximity of the control surface to the vertical tail and outboard engine. The problem was further aggravated by flexibility of the control surface attachment points. Since both analytical calculations show about the same rigid loading, the differences in the calculations with dynamic pressure are attributed to the limited number of modes used in the modal analysis.

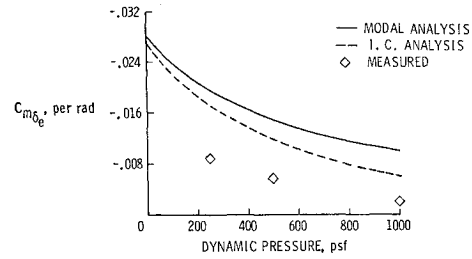

Fig. 8 Effect of dynamic pressure on measured and calculated pitch-control effectiveness at $M = 2.7$.

V. Conclusions

It was the purpose of this paper to present a wind-tunnel evaluation of analytical techniques for predicting the static longitudinal aerodynamic characteristics of a highly flexible

supersonic transport configuration. An examination of the results obtained from both comparative analyses and wind-tunnel studies of a 0.015-size flexibly scaled model indicates that

1) Both analytical methods yield generally accurate results for calculating Mach number and dynamic pressure effects on C_{L_α} and $C_L|_{\alpha=0}$.

2) Both analytical methods predict the effect of dynamic pressure on aerodynamic center movement and $C_m|_{\alpha=0}$, but are somewhat poorer in predicting the absolute level.

3) Prediction of the level of control surface effectiveness was quite poor for both analyses; however, the increment in control surface effectiveness with dynamic pressure is predicted somewhat better.

References

[1] Roskam, J., Holgate, T., and Shimizu, G., "Elastic Wind Tunnel Models for Predicting Longitudinal Stability Derivatives of Elastic Airplanes," *Journal of Aircraft*, Vol. 5, No. 6, Nov.–Dec. 1968, pp. 543–550.

[2] Dusto, A., Chevalier, H., Dornfeld, G., and Schwanz, R., "An Analytical Method for predicting the Stability and Control Characteristics of Large Elastic Airplanes at Subsonic and Supersonic Speeds, Part I—Analysis Part II—Application," Paper presented at *34th Meeting of the AGARD Flight Mechanics Panel*, Marseilles, France, April 1969.

[3] Wykes, J. H. and Lawrence, R. E., "Aerothermoelasticity: Its Impact on Stability and Control of Winged Aerospace Vehicles," *Journal of Aircraft*, Vol. 2, No. 6, Nov.–Dec. 1965, pp. 517–526.

[4] Gauzy, H. "Measurement of Inertia and Structural Damping," *AGARD Manual on Aeroelasticity*, Vol. IV, Oct. 1968.

[5] "Aeroelasticity Summary Report Boeing Model 2707," D6A10626-1, Feb. 1968, The Boeing Co., Seattle, Wash.

[6] Watkins, C. E. Woolston, D. S., and Cunningham, H. J., "A Systematic Kernel Function Procedure for Determining Aerodynamic Forces on Oscillating or Steady Finite Wings at Subsonic Speeds," TR R-48, 1959. NASA.

[7] Donato, V. W. and Huhn, C. R., "Supersonic Unsteady Aerodynamics for Wings With Trailing Edge Control Surfaces and Folded Tips," AFFDL-TR-68-30, Aug. 1968, Air Force Flight Dynamics Lab.

[8] Woodward, F. A., Tinoco, E. N., and Larsen, J. W., "Analysis and Design of Supersonic Wing-Body Combinations, Including Flow Properties in the Near Field, Part I—Theory and Application," CR-73106, 1967, NASA.